J Solid State Electrochem (2006) 10: 125–133
DOI 10.1007/s10008-005-0054-2

ORIGINAL PAPER

G. Inzelt · Z. Puskàs

Electrochemical nanogravimetric study on the ruthenium(III) trichloride–polyaniline nanocomposite

Received: 8 June 2005 / Accepted: 1 July 2005 / Published online: 2 September 2005

Abstract Ruthenium(III) trichloride microcrystals were soaked in aniline and aniline/acetonitrile mixtures. In all cases, polyaniline (PANI) was formed as a result of the intercalation of aniline into the layered structure of $RuCl_3$ crystal and the reaction between aniline and the host material. The appearance of polyaniline was proven by infrared spectroscopy. The as-formed $(PANI)_x^{z+}(RuCl_3)_y^{z-}$ nanocomposites were attached to gold surfaces and studied by cyclic electrochemical nanogravimetry. The sorption of aniline and its effect on the nanocomposites immobilized on gold were also studied in supporting electrolytes. The redox behaviour of the composite shows the electrochemical transformations of both polyaniline and $RuCl_3$. The redox waves of PANI are similar to those observed for very thin PANI films. It attests that the response is originated from monolayer-like PANI film situated between $RuCl_3$ layers. The transport of the charge-compensating ions reflects the variation of the oxidation states of both PANI and $RuCl_3$. The nanocomposites behave as self-doped layers in the potential region when both constituents are charged, i.e. PANI is partially oxidized while $RuCl_3$ is partially reduced, since the electroneutrality is assured by mutual charge compensation. When PANI is reduced, cations enter the layer to counterbalance the negative charge resulting from the reduction of Ru(III) to Ru(II). It was also found that the intercalation of water molecules is—albeit still substantial—smaller than that of pure $RuCl_3$ microcrystals, which is related to the presence of PANI between the $RuCl_3$ layers.

Keywords Ruthenium(III) chloride · Microcrystals · Polyaniline · Intercalation · Electrochemical quartz crystal microbalance

Dedicated to Prof. Mikhail A. Vorotyntsev on the occasion of his 60th birthday

G. Inzelt (✉) · Z. Puskàs
Department of Physical Chemistry, Eötvös Loránd University, Budapest, Pázmány Péter sétány 1/A 1117, Hungary
E-mail: inzeltgy@para.chem.elte.hu
Tel.: +36-1-2090555
Fax: +36-1-3722548

Introduction

Lamellar nanocomposites consisting of layered inorganic compounds and conducting polymers display novel properties which result from the molecular level interaction of two dissimilar chemical components [1–6]. Intercalative polymerization of aniline in α-$RuCl_3$ host has been reported recently [1, 2]. The insertion of aniline into α-$RuCl_3$ has been executed from a solution of aniline in acetonitrile. It has been proven that polyaniline was formed between the $RuCl_3$ layers, which are composed of hexagonal sheets of Ru atoms sandwiched between two hexagonal sheets of Cl atoms with ABC stacking. In the Ru sheets, one-third of the positions are left unoccupied [1, 2, 7–13]. The $RuCl_3$ is a strongly oxidizing host which can take up the electrons from the aniline leading to the formation of polyaniline (PANI). Simultaneously, a fraction of Ru^{3+} atoms is reduced to Ru^{2+}, resulting in a mixed valence compound [1, 2]. The host material will have a negative charge, and $RuCl_3^-$ sites can act as counterions for anilinium cations and charged PANI in the nanocomposite, $(PANI)_x^{z+}(RuCl_3)_y^{z-}$. The X-ray diffraction pattern of the samples revealed that the structure of the inorganic host was preserved; however, a $\Delta d = 0.62$ nm increase in the separation of the $RuCl_3$ layers occurred [1, 2]. It has to be mentioned that the interlayer spacing also increases as a consequence of the intercalation of the hydrated ions during the reduction of α-$RuCl_3$, e.g. $\Delta d = 0.54$ nm (Li^+) or 0.566 nm (Na^+) [10, 11]. The new $(PANI)_x(RuCl_3)_y$ nanocomposite has also been characterized by thermogravimetric analysis, infrared spectroscopy, magnetic measurements as well as electrical and ionic conductivities and thermopower measurements [1, 2]. It has been established that the charge transport—which occurs by electron hopping between the ruthenium ions in the mixed-valent compound—is substantially enhanced by the presence of the conductive polymer. The results of the thermopower study indicate a bulk metal-like conductivity which is controlled by the conductive polymer. $(PANI)_x(RuCl_3)_y$ shows a room temperature conductivity of ca. 1 S cm^{-1} [2]. It was suggested that the combination of the high conductivity of polyaniline [14–17] and the wide-ranging catalytic properties of $RuCl_3$ [7–9, 18–20] could provide new materials with valuable electrocatalytic properties [1, 2].

A logical continuation of these efforts is the study of the redox behaviour of this nanocomposite by electrochemical methods including the investigation of the ionic charge transport processes by nanogravimetry since the oxidation state and consequently the properties of the nanocomposite can be tuned electrochemically. In this article, we report the results on the behaviour of $(PANI)_x(RuCl_3)_y$ nanocomposite prepared in different ways. The microcrystals were immobilized at gold surfaces [21–23] and studied by electrochemical quartz crystal microbalance technique.

Experimental

Black-coloured $RuCl_3$ microcrystals, HCl, NaCl, aniline (Merck, analytical grade) and doubly distilled water were used. In the EQCM measurements, 10 MHz AT-cut crystals coated with gold were used. The detailed description of the apparatus and its calibration have been published in our previous papers [24–27]. The geometrical and piezoelectrically active area of the working electrode was 0.4 cm^2. A Pt wire was used as a counter-electrode. The reference electrode was a saturated sodium calomel electrode (SCE). All potentials are referred to SCE. The $(PANI)_x(RuCl_3)_y$ samples were prepared in three different ways. First, the procedure described in [1, 2] was used, i.e. 0.1 g $RuCl_3$ was added to 10 cm^3 of 4% aniline/acetonitrile solution; the suspension was stored for 5–7 days and occasionally stirred. The product [labelled $(PANI)_x(RuCl_3)_y$ (A)] was washed with acetonitrile and dried. Second, the same procedure was followed except pure aniline was added to the $RuCl_3$ microcrystals and HCl was used to wash the resulting material (labelled B). Third, nanocomposites A and B attached to gold were investigated by electrochemical quartz crystal microbalance in the presence of HCl or NaCl solutions and then aniline was added to the solution. The incorporation of aniline was detected by measuring the frequency change. The nanocomposite formed (marked as C) was investigated further on when practically no more frequency decrease could be observed.

The microcrystals were attached to the gold surface by placing the material on the electrode [24–27] and then, making use of a drop of water, the microcrystals were fixed. Although $RuCl_3$ and $(PANI)_x(RuCl_3)_y$ microcrystals were found to be insoluble in water, using this procedure the crystals can be "glued" to the metal. This method of preparing the electrode produces a randomly distributed ensemble of microcrystals on gold; however, the distribution of microcrystals was more or less uniform. Although the requirements (uniform and homogeneous surface layer) for the application of Sauerbrey equation are not perfectly met, on the basis of measured frequency values (Δf) a rough estimation can be done. The relative values of Δf obtained for the incorporation of aniline or different ions and solvent molecules, however, should be approximately correct. Therefore, Sauerbrey equation was used for the calculation of the surface mass changes (Δm) from the frequency changes (Δf), with an integral sensitivity [$C_f = (1.9 \pm 0.2) \times 10^8$ Hz cm^2 g^{-1}] that was determined in separate experiments [27]. The amount of $RuCl_3$ and $(PANI)_x(RuCl_3)_y$ immobilized on the surface (0.5–15 μg) was estimated by measuring the crystal frequency before and after the deposition in dry state. Solutions of different concentrations of HCl and NaCl were used. The measurements were carried out at 25°C. All solutions were purged with oxygen-free argon and an inert gas blanket was maintained throughout the experiments.

An Elektroflex 453 potentiostat and an Universal Frequency Counter TR-5288 connected with an IBM personal computer were used for the control of the measurements and for the acquisition of data. $(PANI)_x(RuCl_3)_y$ nanocomposites as pressed KBr pellets were investigated by infrared (FTIR) transmission spectroscopy using a Bruker IFS-55 Fourier Transform Spectrometer.

Results and discussion

Figure 1 shows the cyclic voltammograms obtained for $RuCl_3$ and $(PANI)_x(RuCl_3)_y$ (B) samples attached to a gold electrode and studied in the presence of 0.5 mol dm^{-3} HCl.

In these experiments, first pure α-$RuCl_3$, then $(PANI)_x(RuCl_3)_y$ (B) prepared by 1-week-long soak of α-$RuCl_3$ microcrystals in aniline were immobilized at the gold surface. The nanocomposite was washed with 0.5 mol dm^{-3} HCl before use. A comparison of the cyclic voltammograms displayed in Fig. 1a reveals that the oxidation of Ru^{2+} to Ru^{3+} becomes easier since wave II moves into the direction of lower potentials while the reduction process remains unaltered. It may be related to the presence of polyaniline, which is conducting in this potential region, and probably enhances the charge transfer processes. The waves belonging to the leucoemeraldine (LE)$\rightleftarrows$emeraldine (E) transition are clearly seen in Fig. 1a (waves III and IV). We can assign these waves to the redox transformations of polyaniline since the peak potentials are close to those observed for PANI films in this media [14, 28]. Figure 1b shows the cyclic voltammograms obtained at a slow scan rate in the whole potential region and where the redox transformations of $RuCl_3$ play no role, i.e. the response of

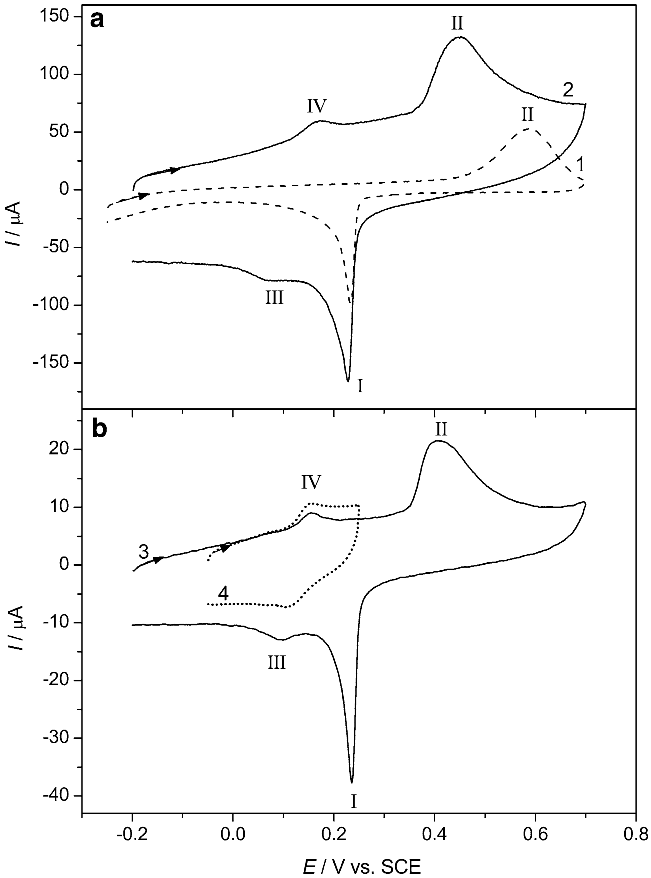

Fig. 1 Cyclic voltammograms obtained at different scan rates **a** $v = 50$ mV s^{-1} and **b** $v = 5$ mV s^{-1} for Au|$RuCl_3$ (*curve 1*) and Au|$(PANI)_x$ $(RuCl_3)_y$ (B) (*curves 2, 3, 4*). Electrolyte: 0.5 mol dm^{-3} HCl

PANI can be seen separately. An even more direct proof regarding the formation of polyaniline is furnished by the IR spectra. The IR spectrum obtained for the sample used in the experiments described above is shown in Fig. 2. Almost all peaks in the IR spectrum of $(PANI)_x(RuCl_3)_y$ presented in Fig. 2 are associated with the

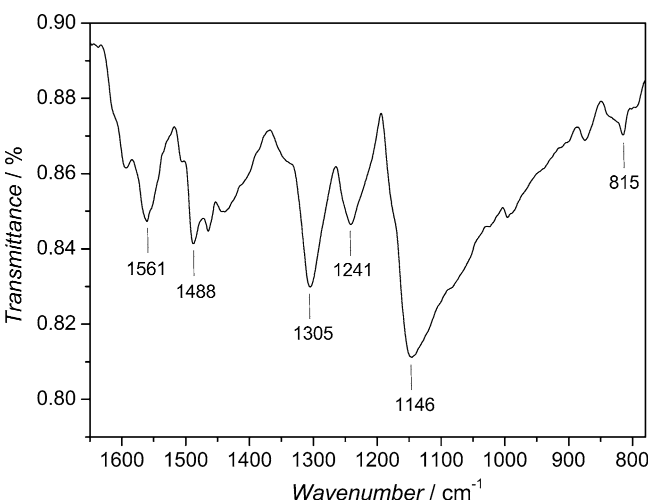

Fig. 2 Infrared spectra of $(PANI)_x(RuCl_3)_y$ (B)

emeraldine salt form of polyaniline. In the previous publications similar spectra have been reported [2, 29–36]. The characteristic vibration bands can be assigned as follows: benzoid ring (1,561 cm^{-1}), quinoid ring (1,488 cm^{-1}), –C–N stretch (1,305 and 1,241 cm^{-1}), –C–H in plane (1,146 cm^{-1}), –C–H out of plane (815 cm^{-1}).

The electrode used in the experiments presented in Fig. 1 was soaked in a solution containing 0.4 mol dm^{-3} aniline and 0.2 mol dm^{-3} HCl for 3 h (nanocomposite C). The cyclic voltammogram shown in Fig. 3a (curve 1) clearly indicates the additional deposition of PANI which means that $RuCl_3$ was still able to oxidize aniline and enhance the formation of PANI. In order to ascertain that the redox behaviour originated from PANI, some layers of PANI were electropolymerized on top of the crystals as shown in Fig. 3b. The cyclic voltammetric curves obtained before (curve 1) and after (curve 2) the electropolymerization are displayed in Fig. 3a. The comparison reveals that there is no doubt that the original response is also due to the PANI redox transformations.

The electrochemical activity of PANI decreases with increasing pH [37, 38], and at pH > 5—except for self-doped films [35, 36, 39–43]—no redox response can be observed. Therefore, we have tried whether the $(PANI)_x(RuCl_3)_y$ composite behaves as a self-doped system or not. Figure 4 shows the voltammograms of the nanocomposite B in the presence of 0.5 M HCl and 0.5 M NaCl, respectively. Although both waves belonging to $Ru^{3+} \rightarrow Ru^{2+}$ and LE $\rightarrow$ E transition, respectively, move into the direction of higher potentials, it is clearly seen that the electrochemical activity (see waves III and IV) of PANI was preserved. The sharp pair of waves at low potentials is a typical response of α-$RuCl_3$ in neutral salt solutions [44]. Its nature has been discussed recently [44]; however, the presence of PANI certainly enhances this process.

The scan rate dependence shown in Fig. 5 attests that the redox transformations of both ruthenium and polyaniline are fast; however, the mass changes accompanying the redox reactions somewhat decrease with increasing scan rate. All the waves behave as surface waves at low scan rates since the peak currents are proportional to the scan rate; however, an interplay between the surface and diffusional behaviour can be observed at $v >$ ca. 50 mV s^{-1}, and eventually a diffusional response develops.

When aniline was added to the solution at open circuit ($E = 0.21$ V), a fast frequency decrease was observed as shown in Fig. 6. It is somewhat surprising since the sample attached to the gold surface had been soaked in an aniline-containing solution and showed the presence of PANI (see Figs. 1, 4, 5). The amount of aniline adsorbed/absorbed was 2.6×10^{-7} g, which means that the resulting layer contains ca. 1 mol aniline/1 mol $RuCl_3$. The mass increases/decreases in the course of subsequent potential steps were in accordance with those observed in cyclic voltammetric experiments. During the potential step investigations the potential region where aniline

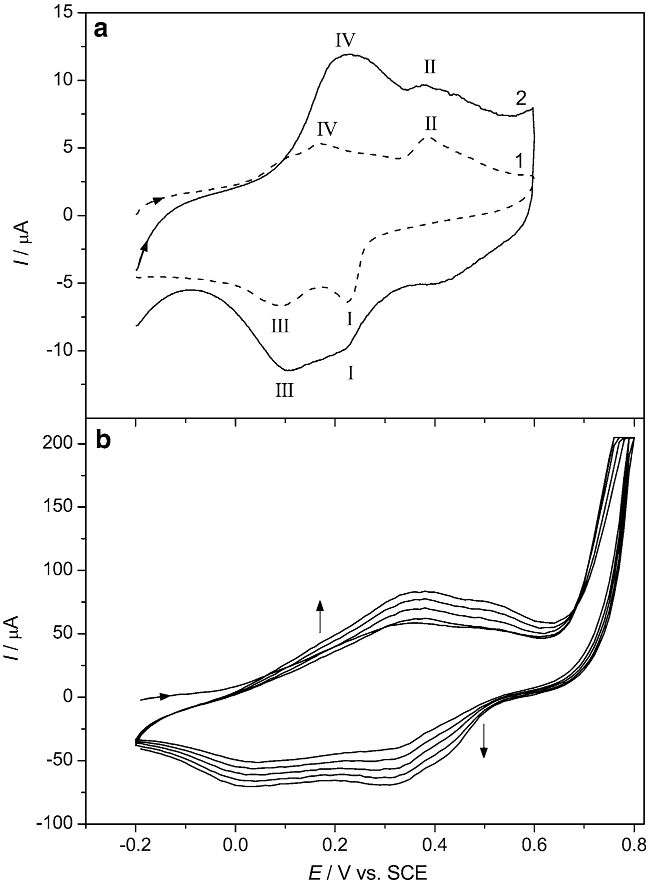

Fig. 3 Cyclic voltammograms of Au|$(PANI)_x(RuCl_3)_y$ (C) electrodes **a** after soaking the electrode used in Fig. 1 in a solution containing 0.4 mol dm^{-3} aniline and 0.2 mol dm^{-3} HCl for 3 h (*curve 1*); the cyclic voltammogram taken after the electropolymerization shown in (**b**) (*curve 2*). Electrolyte: 0.5 mol dm^{-3} HCl, scan rate: 5 mV s^{-1}. **b** Electropolymerization of aniline by potential cycling between −0.2 and +0.8 V versus SCE on the $(PANI)_x(RuCl_3)_y$ (C) electrode used in the experiment shown in *curve 1* of **a**. Solution: 0.4 mol dm^{-3} aniline + 0.2 mol dm^{-3} HCl; scan rate: 50 mV s^{-1}

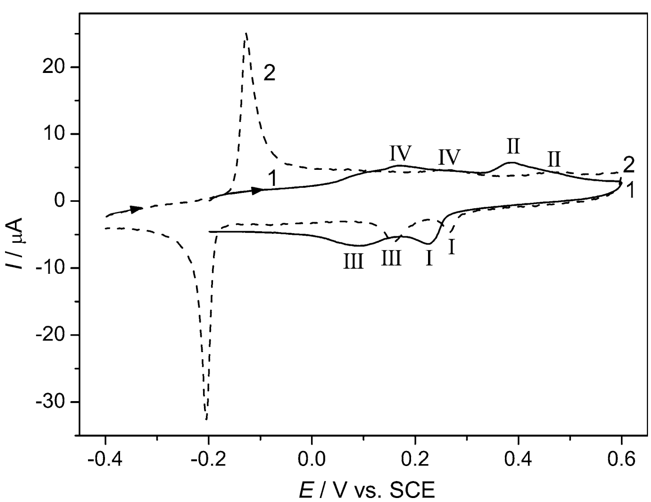

Fig. 4 Cyclic voltammetric curves obtained for a Au|$(PANI)_x$ $(RuCl_3)_y$ (B) electrode in the presence of (*1*) 0.5 mol dm^{-3} HCl and (*2*) 0.5 mol dm^{-3} NaCl. Scan rate: 5 mV s^{-1}

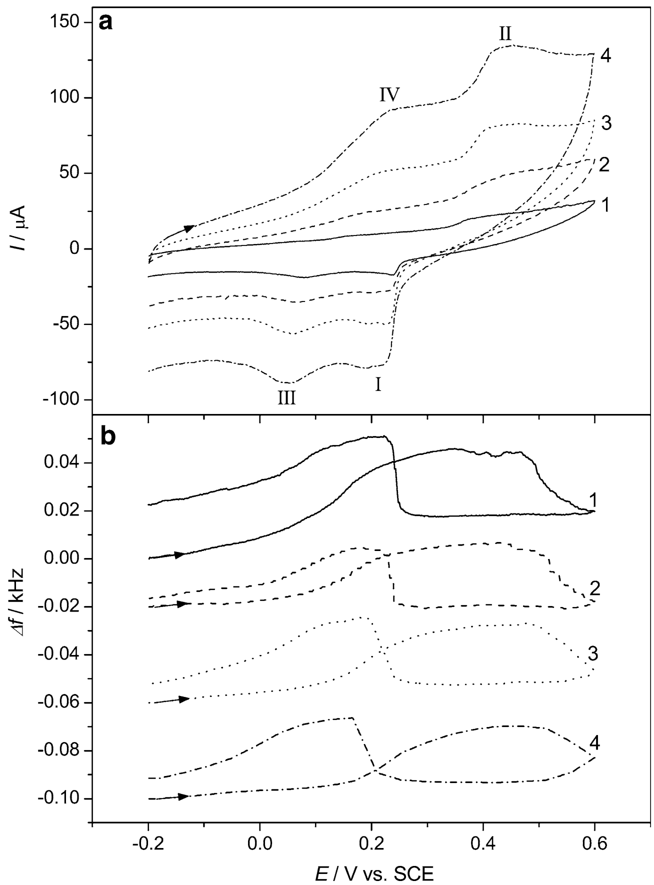

Fig. 5 The effect of scan rate on **a** the cyclic voltammograms and **b** the simultaneously detected EQCM frequency curves obtained for a Au|$(PANI)_x(RuCl_3)_y$ (B) electrode. Scan rates are (*1*) 5, (*2*) 20, (*3*) 50 and (*4*) 100 mV s^{-1}. Electrolyte: 0.5 mol dm^{-3} HCl

electropolymerization could have occurred was avoided. In Fig. 7 the cyclic voltammetric and microgravimetric responses before (nanocomposite B) and after the addition of aniline (nanocomposite C), respectively, are compared. The anodic part of the voltammogram became more drawn-out, and the cathodic waves shift to higher potentials. Even more drastic changes of the EQCM frequency curves can be observed. The steep frequency increase at the reduction wave of Ru^{3+} disappeared and a rather reversible frequency variation can be observed. Since this frequency increase has been assigned to the desorption of water molecules [24, 44], we may conclude that aniline molecules replaced water molecules within the interlayer space. It should be mentioned that potential cycling in the presence of aniline and HCl for a longer period of time—in the potential region where electropolymerization does not take place—leads to an excessive insertion of aniline (anilinium chloride), which eventually decreases the electrochemical activity of the layer. It may be related to the diminishing charge transfer between the $RuCl_3$ layers.

The behaviour of the $(PANI)_x(RuCl_3)_y$ samples produced by different treatments has also been compared. The voltammetric and EQCM responses of the layers prepared in aniline (nanocomposite B) (presented in

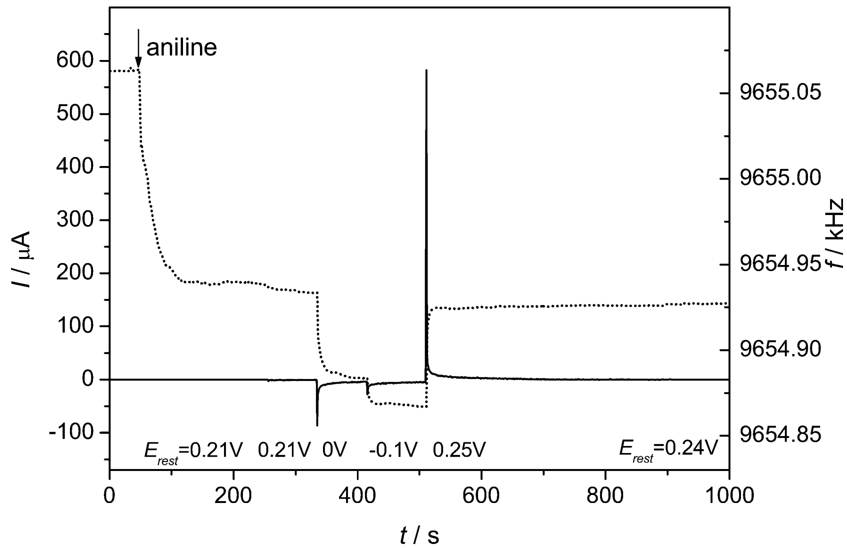

Fig. 6 Sorption of aniline in the $(PANI)_x(RuCl_3)_y$ (B) layer attached to the gold surface. The moment of the addition of aniline to the 0.5 mol dm^{-3} HCl supporting electrolyte is indicated by an *arrow*. Frequency changes (*dotted line*) and current responses (*continuous line*) in the course of the open circuit and the subsequent potential step experiments are shown

Figs. 4, 5, 7) and in aniline/acetonitrile solution (nanocomposite A), respectively, are shown in Fig. 8. The latter $(PANI)_x(RuCl_3)_y$ (A) nanocomposite displays a more reversible behaviour especially regarding the reoxidation of Ru^{2+} (wave II). The mass change is also more regular in as much as there are no crossed curves. Furthermore, at lower potentials a mass increase and decrease during oxidation and reduction, respectively, can be observed, while it was just the opposite in the case of the nanocomposite layer prepared without acetoni-

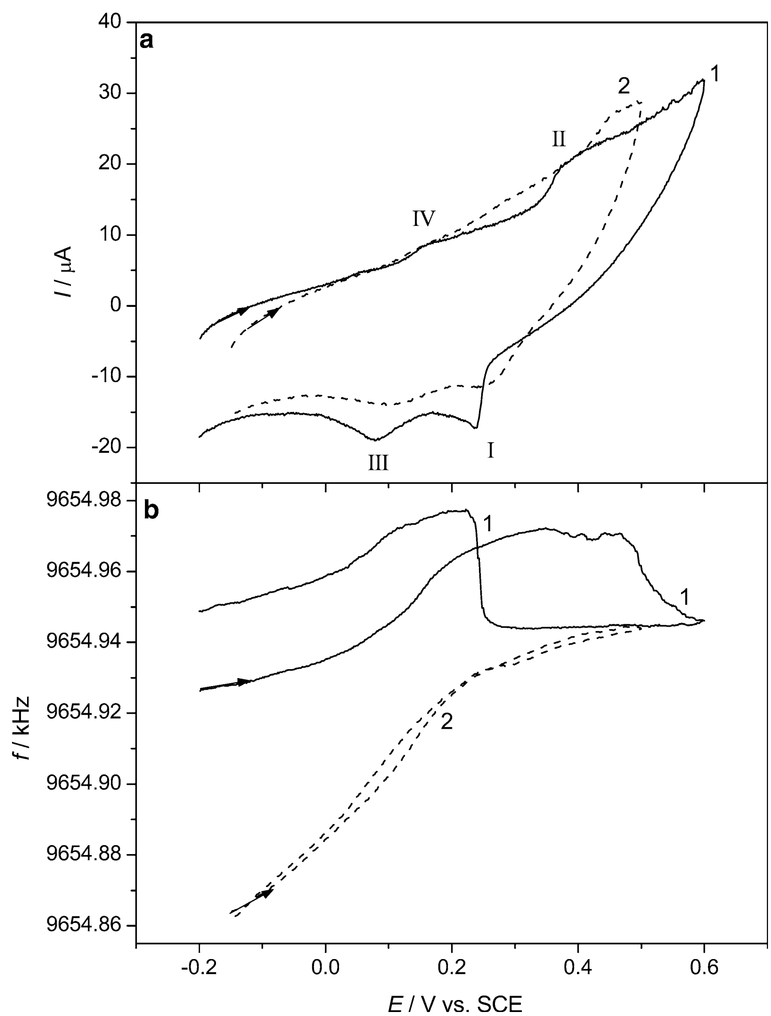

Fig. 7 A comparison of **a** the cyclic voltammetric and **b** the simultaneously obtained EQCM frequency responses before (nanocomposite B, *curve 1*) and after the addition of aniline (nanocomposite C, *curve 2*) the experiment of which is presented in Fig. 6. Electrolyte: 0.5 mol dm^{-3} HCl, scan rate: 5 mV s^{-1}

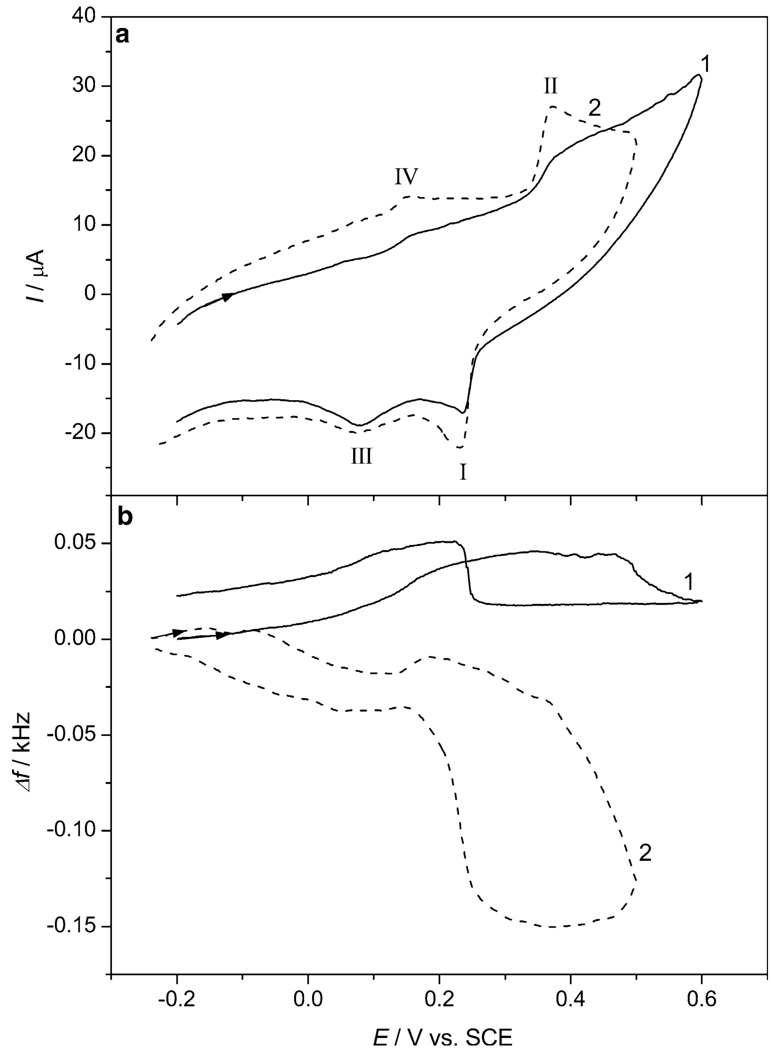

Fig. 8 A comparison of **a** the cyclic voltammetric and **b** the EQCM frequency responses of two Au|$(PANI)_x(RuCl_3)_y$ electrodes. The nanocomposites were prepared in $RuCl_3$–aniline (nanocomposite B, *curve 1*) and in $RuCl_3$–aniline–acetonitrile (nanocomposite A, *curve 2*) suspensions, respectively. Electrolyte: 0.5 mol dm^{-3} HCl, scan rate: 5 mV s^{-1}

trile. Another important feature is the much higher frequency change at the $Ru^{3+} \rightleftarrows Ru^{2+}$ transitions. In order to clarify the nature of the mobile species causing the mass increase and decrease phenomena the Au|$(PANI)_x(RuCl_3)_y$ (A) electrode has been studied in perchloric acid media also. As seen in Fig. 9 there is only a slight change in the voltammetric response and—as expected—a higher mass change occurs in the presence of ClO_4^- ions in comparison with that of Cl^- ions. However, the variation is much below the theoretical $M(ClO_4^-)/M(Cl^-) = 2.8$ molar ratio. From the slope of the $\Delta f(\Delta m)$ versus Q plots the apparent molar masses were calculated, which gave $M_{app}(ClO_4^-) = 124 \pm 15$ and $M_{app}(Cl^-) = 94 \pm 15$, respectively.

Although this discrepancy may be explained by the higher hydration of chloride ions, i.e. chloride ions transfer more water molecules, it is likely that the phenomena observed are not related to the sorption and desorption of anions. The results obtained for α-$RuCl_3$ microcrystals indicate that at peak I a phase transition occurs which is accompanied by the desorption of water molecules, and cations enter the solid phase during the reduction [22, 44]. The different behaviours of nanocomposites A and B (Fig. 8) as well as the effect of excess aniline support the idea that the structural changes of α-$RuCl_3$ play a decisive role in the behaviour of the layer including the sorption/desorption of mobile species. The most versatile behaviour is expected concerning the incorporation of neutral molecules since it is only indirectly affected by the charging state of the solid phase. Nevertheless, we should not exclude anion sorption at high potentials since the Ru^{III} Cl_3 cannot act as counterions. At low potentials the reduced PANI cannot compensate the negative charge of the reduced Ru^{II} Cl_3^- sites; therefore, the incorporation of cations in partially hydrated form is expected. In acidic solutions PANI may posses positive charge due to its protonation (protonated LE form) [28, 45, 46]; however, it is sufficient to maintain the electroneutrality only in the case when $x = y$ and PANI is fully protonated. From the charge consumed in the course of the cyclic voltammetric experiments a rough estimation can be made for the x/y ratio in the $(PANI)_x(RuCl_3)_y$ nanocomposites. For the nanocomposites A and B this ratio is 0.5–0.9 and 0.3–0.8, respectively, depending on the preparation conditions. By the treatment in aniline–HCl solutions,

Fig. 9 The effect of the anions on **a** the cyclic voltammetric and **b** EQCM responses. Au|$(PANI)_x(RuCl_3)_y$ (A) prepared in aniline/acetonitrile solution in contact with (*1*) 0.5 mol dm^{-3} $HClO_4$ (*continuous line*) and (*2*) 0.5 mol dm^{-3} HCl (*dotted line*), respectively. Scan rate: 5 mV s^{-1}. **c** The frequency is plotted as a function of the charge consumed (*Q*)

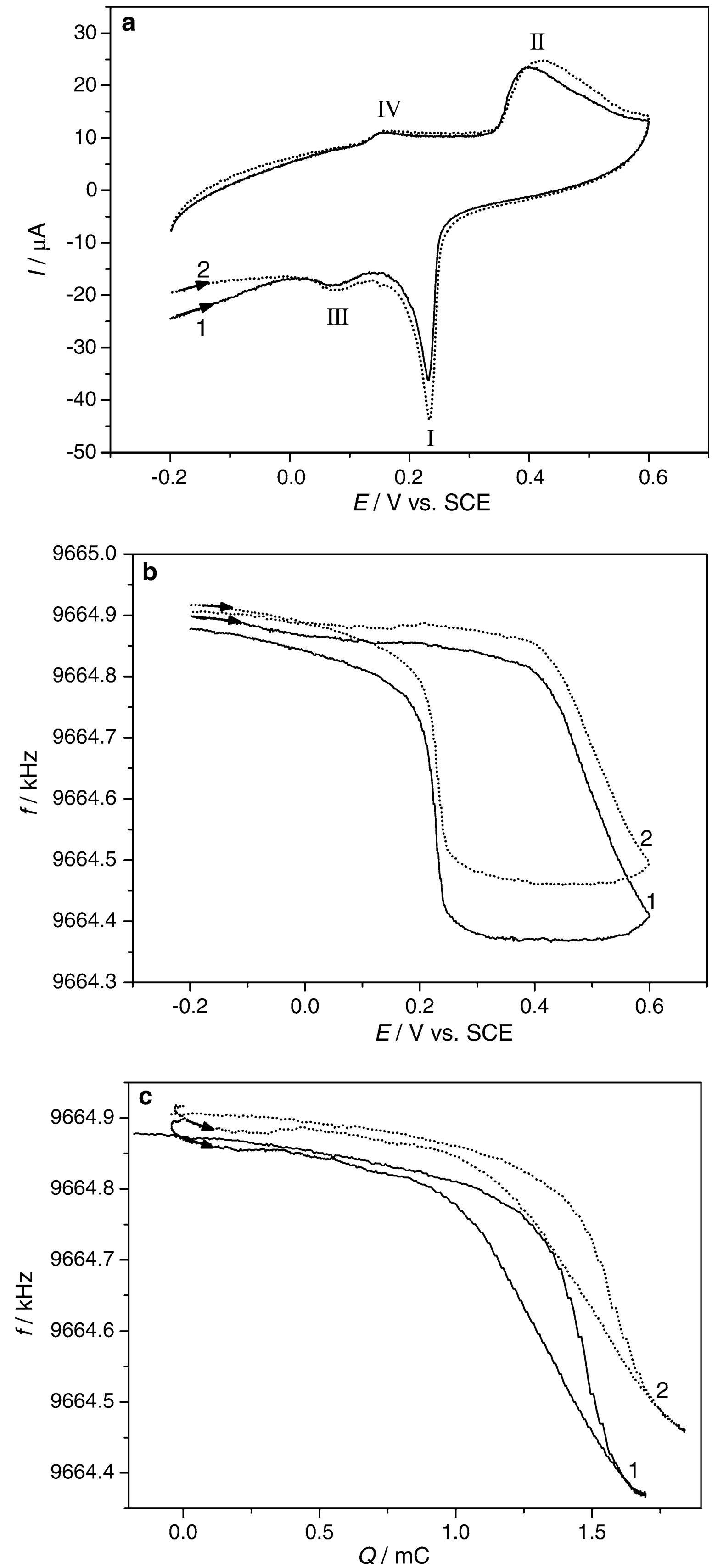

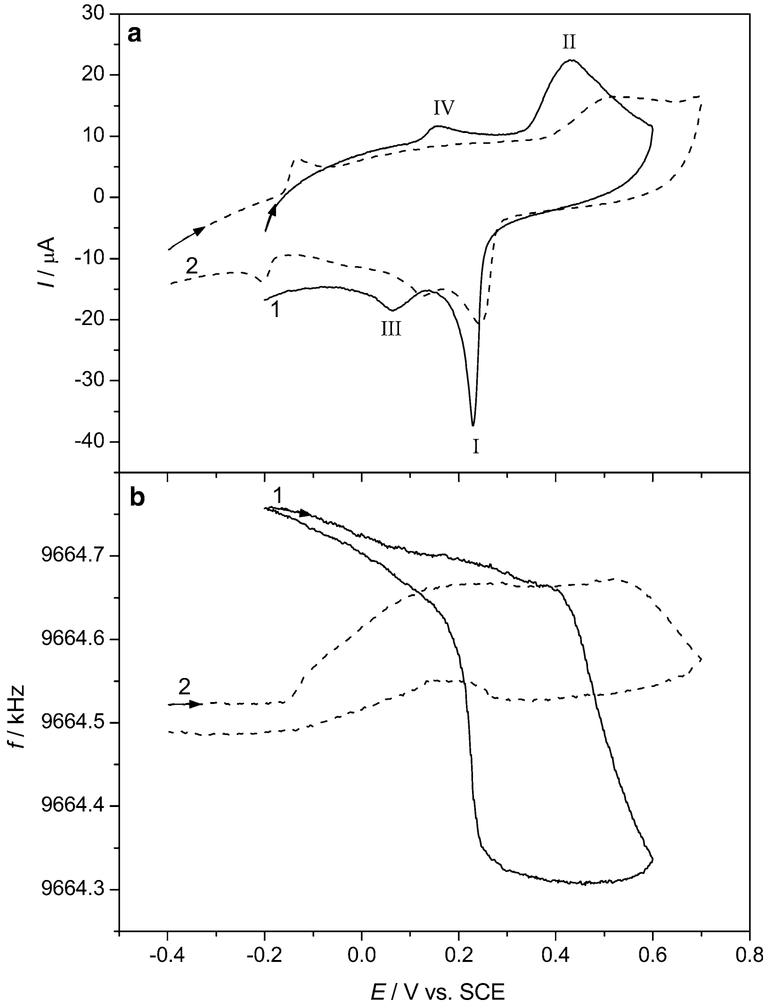

Fig. 10 Cyclic voltammetric (**a**) and EQCM responses (**b**) obtained for $(PANI)_x(RuCl_3)_y$ (A) nanocomposite in the presence of 0.5 mol dm^{-3} HCl (*1*) and 0.5 mol dm^{-3} NaCl (*2*), respectively. Scan rate: 5 mV s^{-1}

$x/y \sim 1$ can be achieved (see Fig. 3a); however, further incorporation of anilinium ions eventually destroys the structure of the microcrystals that leads to the decrease of the electroactivity. In HCl electrolytes only H^+ (or H_3O^+) ions can enter the nanocomposite or alternatively H^+ ions insertion occurs and water molecules leave the film. In the first case, only a rather small frequency decrease is expected, while in the second case even frequency increase can be observed depending on the extent of counterflux of the mobile species. On the other hand, in NaCl solutions a more distinct mass increase has to be observed due to a factor of 23 in the molar masses of Na^+ as compared to H^+. As seen in Fig. 10 it happens indeed, although the picture is somewhat complicated due to a second reduction process of $RuCl_3$ in neutral media.

Conclusions

The results of the electrochemical microgravimetry support the previous findings [1, 2] that aniline molecules can be intercalated in the lamellar structure of α-$RuCl_3$. Ru^{3+} ions oxidise aniline molecules resulting in the formation of polyaniline monolayers within the gallery space of $RuCl_3$. The properties of the $(PANI)_x^{z+}(RuCl_3)_y^{z-}$ nanocomposite somewhat depend on the method of preparation; however, in all cases the electrochemical responses clearly show the redox responses of both leucoemeraldine $\rightleftarrows$ emeraldine and $Ru^{3+} \rightleftarrows Ru^{2+}$ transitions. The results of electrochemical nanogravimetric studies can be explained by the sorption/desorption of ionic species and water molecules. The degree of the solvent sorption/desorption is affected by the method of preparation. The nanocomposites prepared by using a solution containing aniline and acetonitrile show a more regular behaviour than those when only pure aniline was in contact with $RuCl_3$. In the presence of an aqueous solution of HCl and aniline a higher degree of aniline incorporation can be achieved. It also attests that the morphology of the layer is influenced by the contacting media. It has also been observed, however, that cycling for a longer period of time in the presence of aniline and HCl causes a decrease in the electrochemical activity of the layer. It is related to the high degree of swelling of the layer, which hinders the charge transfer between the $RuCl_3$ sites. The nanocomposite behaves as a self-doped conducting polymeric system where $RuCl_3^{x-}$ sites act as counterions; however, cation sorption/desorption is inevitable when PANI becomes fully reduced in order to compensate the negative charge of $RuCl_3^{x-}$. In a smaller extent anion transport also takes place. The self-doped nature of the conducting polymer manifests itself so that PANI remains electroactive even in neutral solutions.

Acknowledgements Financial support by the National Scientific Research Fund (OTKA T046987) is gratefully acknowledged. The authors express their thanks to G. Magyarfalvi for his help in the FTIR measurements.

References

1. Wang L, Brazis P, Rocci M, Kannewurf CR, Kanatzidis MG (1998) Chem Mater 10:3298
2. Wang L, Rocci-Lane M, Brazis P, Kannewurf CR, Kim YI, Lee W, Choy JH, Kanatzidis MG (2000) J Am Chem Soc 122:6629
3. Alberti G, Bein T (eds) (1996) Comprehensive supramolecular chemistry, vol 7. Elsevier, New York
4. Gianellis EP (1996) Adv Mater 8:29
5. Leroux F, Goward G, Power WP, Nazar LF (1997) J Electrochem Soc 144:3886
6. Wang Y, Herron N (1996) Science 273:632
7. Cotton FA, Wilkinson G, Murillo CA, Bochman M (1999) Advanced inorganic chemistry. Wiley, New York, pp 1010–1039
8. Livingstone SE (1973) In: Bailar JC, Emeléus MJ, Nyholm R, Trotman-Dickenson AF (eds) Comprehensive inorganic chemistry, vol 3. Pergamon, Oxford, pp 1163–1370
9. Chandret B, Sabo-Etienne S (1994) In: King RB (ed) Encyclopedia of inorganic chemistry, vol 7. Wiley, Chichester
10. Schöllhorn R, Steffen R, Wagner K (1983) Angew Chem 95:559
11. Steffen R, Schöllhorn R (1986) Solid State Ionics 22:31
12. Pollini I (1994) Phys Rev B 50:4
13. Pollini I (1996) Phys Rev B 53:19
14. Inzelt G, Pineri M, Schultze JW, Vorotyntsev MA (2000) Electrochim Acta 45:2403
15. Paul EW, Ricco AJ, Wrighton MS (1985) J Phys Chem 89:1441
16. Csahók E, Vieil E, Inzelt G (2000) J Electroanal Chem 482:168
17. Probst M, Holze R (1995) Electrochim Acta 40:213
18. Appelbaum L, Heinrichs C, Demtschuk J, Michman M, Oron M, Schäfer HJ, Schumann H, (1999) Organomet J Chem 592:240
19. Llopis JF, Tordesillas IM (1976) In: Bard AJ (ed) Encyclopedia of electrochemistry, vol 6. Marcel Dekker, New York, p 277
20. Colom F (1985) In: Bard AJ, Parsons R, Jordan J (eds) Standard potentials in aqueous solution. Marcel Dekker, New York, p 413
21. Scholz F, Meyer B (1998) In: Bard AJ, Rubinstein I (eds) Electroanalytical chemistry, vol. 20. Marcel Dekker, New York, p 1
22. Grygar T, Marken F, Schröder U, Scholz F (2002) Cell Czech Chem Commun 67:163
23. Fiedler DA, Scholz F (2002) In: Scholz F (ed) Electroanalytical methods, chap II, vol 8. Springer, Berlin Heidelberg New York, pp 201–222
24. Inzelt G, Puskás Z (2004) Electrochem Commun 6:805
25. Fehér K, Inzelt G (2002) Electrochim Acta 47:3551
26. Inzelt G (2003) J Solid State Electrochem 7:503
27. Inzelt G, Puskás Z (2004) Electrochim Acta 49:1969
28. Bácskai J, Kertész V, Inzelt G (1993) Electrochim Acta 38:393
29. Habib MA, Maheswari SP (1989) J Electrochem Soc 136:1050
30. Seeger D, Kowalchyk W, Korzeniewski C (1990) Langmuir 6:1527
31. Ping Z, Nauer GE, Neugebauer H, Theiner J, Neckel A (1997) J Chem Soc Faraday Trans 93:121
32. Zimmermann A, Künzelman U, Dunsch L (1998) Synth Met 93:17
33. Hatchett DW, Josowicz M, Janata J (1999) J Electrochem Soc 146:4535
34. Maia DJ, Das Neves S, Alves OL, De Paoli MA (1999) Electrochim Acta 44:1945
35. Barbero C, Miras MC, Haas O, Kötz R (1997) J Electrochem Soc 144:4170
36. Varela H, Torresi RM, Buttry DA (2000) J Braz Chem Soc 11:32
37. Kalaji M, Nyholm L, Peter LM (1991) J Electroanal Chem 313:271
38. Pruneanu S, Csahók E, Kertész V, Inzelt G (1998) Electrochim Acta 43:2305
39. Orata D, Buttry DA (1998) J Electroanal Chem 257:71
40. Malinauskas A, Holze R (1998) Electrochim Acta 43:515
41. Varela H, Albuquerque Maranho SL, Mello RMQ, Ticianelli EA, Torresi RM (2001) Synth Met 122:321
42. Ding H, Park SM (2003) J Electrochem Soc 150:E33
43. Bauermann LP, Bartlett PN (2005) Electrochim Acta 50:1537
44. Inzelt G, Puskás Z, Németh K, Varga I (2005) J Solid State Electrochem (in press)
45. Vorotyntsev MA, Daikin LI, Levi MD (1994) J Electroanal Chem 364:37
46. Gabrielli C, Keddam M, Nadi N, Perrot H (1999) Electrochim Acta 44:2095